RESEARCH ARTICLE

A combination of monosodium glutamate and high-fat and high-fructose diets increases the risk of kidney injury, gut dysbiosis and host-microbial co-metabolism

Thatsanapong Pongking[1,2,6], Ornuma Haonon[3,6], Rungtiwa Dangtakot[1,6], Sudarat Onsurathum[3,6,7], Apinya Jusakul[2,6], Kitti Intuyod[3,6], Arunnee Sangka[2,6], Sirirat Anutrakulchai[4,6], Ubon Cha'on[5,6], Somchai Pinlaor[3,6], Porntip Pinlaor[iD][2,6]*

1 Biomedical Science Program, Graduate School, Khon Kaen University, Khon Kaen, Thailand, 2 Centre for Research and Development of Medical Diagnostic Laboratories, Faculty of Associated Medical Sciences, Khon Kaen University, Khon Kaen, Thailand, 3 Department of Parasitology, Faculty of Medicine, Khon Kaen University, Khon Kaen, Thailand, 4 Department of Medicine, Faculty of Medicine, Khon Kaen University, Khon Kaen, Thailand, 5 Department of Biochemistry, Faculty of Medicine, Khon Kaen University, Khon Kaen, Thailand, 6 Chronic Kidney Disease Prevention in The Northeast of Thailand, Faculty of Medicine, Khon Kaen University, Khon Kaen, Thailand, 7 Department of Microbiology and Parasitology, Faculty of Medical Science, Naresuan University, Phitsanulok, Thailand

* porawa@kku.ac.th

Abstract

Consumption of either monosodium glutamate (MSG) or high-fat and high-fructose (HFF) diets changes the gut microbiome and hence contributes to development of several diseases. In this study, with an emphasis on kidney injury, hamsters were divided into 4 groups as follows: (1) hamsters fed with standard diet (control); (2) hamsters fed with standard diet and MSG in drinking water (MSG); (3) hamsters fed with high-fat and high-fructose diets (HFF), and (4) animals fed MSG+HFF. After 8 months, the animals were used for the study. Despite showing normal kidney function, hamsters fed with MSG+HFF exhibited signs of kidney damage as demonstrated by the highest expression levels of high-mobility group box-1 and kidney injury molecule-1 in kidney tissues, while slight changes of histopathological features in H&E-stained sections and normal levels of creatinine were observed, indicating possible early stages of kidney injury. Sequencing of the microbial 16S rRNA gene revealed that animals fed with the MSG+HFF diet had a higher ratio of gut Firmicutes/Bacteroidetes along with marked changes in abundance and diversity of gut microbiome compared to hamsters fed with MSG or HFF alone. In addition, ^{1}H Nuclear magnetic resonance spectroscopy showed an elevation of urine p-cresol sulfate levels in the MSG+HFF group. These results indicate that consumption of both MSG and HFF increases the risk of kidney injury, induces gut dysbiosis and an increase in the amount of p-cresol sulfate in hamsters.

Introduction

Remarkable changes in dietary behaviors, levels of physical activity and prevalence of noncommunicable diseases have been noticed in the world population particularly in low- and middle-income countries [1, 2]. The prevalence of chronic kidney disease (CKD), an important noncommunicable disease, is also increasing worldwide [3, 4]. In Thailand, the overall prevalence of CKD was 17.5% but was higher in Bangkok and the Northern and Northeastern regions of the country [5]. Risk factors including age, gender, diabetes, hypertension, hyperuricemia, history of kidney stones and the use of traditional medicines, are associated with CKD development [5]. Besides these, poor diet is a key risk factor [6]. For instance, consumption of high-fat and high-sugar diets is widely documented as a risk factor for several chronic diseases including CKD [7]. A diet supplemented with high levels of monosodium glutamate (MSG) is also believed to contribute to kidney injury by increasing reactive oxygen species (ROS)-mediated interstitial fibrosis in renal tubules [8, 9], formation of kidney stones [10], and eventually CKD development [11]. Importantly, intake of MSG, along with high-fat and high-fructose diets (HFF), is common in Thailand [12, 13].

The gut microbiota is a complex microbial community comprised of >100 trillion microbial cells. This microbiota plays an important role in human health and disease [14]. The composition of this microbial population can be affected by several factors including antibiotic use, psychological and physical stresses, age, sex, ethnicity, geography, metabolism, immunity and an individual's diet [15, 16]. Hence, changes in gut microbiota have been considered as important links between diet and chronic disease [6] including CKD [17]. For instance, high consumption of MSG decreases the taxa *Faecalibacterium*, *Megamonas*, *Blautia* in the gut microbiota but leads to an increase of *Collinsella* [18]. Reduction in abundance of *Faecalibacterium* was observed in end-stage CKD patients and was correlated with the reduced estimated glomerular filtration rate in these patients and associated with CKD progression [19]. Long-term consumption of HFF decreases the proportion of Bacteroidetes and increases abundance of both Firmicutes and Proteobacteria in the intestine [20, 21], and eventually leads to increased risk of kidney disease by increasing oxidative stress-induced kidney injury [22, 23]. Besides imbalance of gut microbiota or gut dysbiosis, increases of gut microbiota-derived metabolites including trimethylamine-N-oxide [24], indoxyl sulfate and p-cresol sulfate [25, 26] have been implicated in development and progression of CKD [27].

Although it is well established that the consumption of either MSG or HFF alone affects the gut microbiome and plays a role in kidney disease, it is not known whether consumption of MSG and HFF together enhances severity of kidney injury and gut dysbiosis. In this study, we hypothesized that MSG consumption and an HFF diet, in combination, increase extent of kidney damage and alter the gut microbiome. Accordingly, we aimed to investigate the effect of combined MSG and HFF intake on kidney injury, gut microbiome and gut-derived metabolites in an animal model. This will highlight any risks associated with habitual intake, common in Thailand, of diets high in MSG and HFF, and might be useful in finding strategies for prevention of kidney disease development.

Materials & Methods

Ethics statement and experimental design

The protocol of this study was reviewed and approved by the Animal Ethics Committee of Khon Kaen University (IACUC-KKU-22/63) based on the Ethics of Animal Experimentation of National Research Council of Thailand. The animals were obtained from the Animal Unit of Faculty of Medicine, Khon Kaen University. Forty male 6- to 8-week-old Syrian golden

hamsters (*Mesocricetus auratus*), average body weight 100–120 g, were housed in eight cages of five animals each. Hamsters were maintained under a standard light cycle (12 h dark/light) and provided with *ad libitum* access to water and food. To avoid bacterial contamination, the stainless-steel cages were washed twice a week with Sunlight detergent (Unilever, Thailand), decontaminated using the antimicrobial reagent Dettol (Dettol, Thailand) and sawdust was changed 3–4 times per week. Hamsters were assigned into four groups, each consisting of 10 animals, and treated as follows for 8 months; 1) normal control group (fed with normal diet); 2) a group fed a high-fat diet along with 10% fructose added in drinking water (HFF); 3) a group given 20 mg/ml of monosodium glutamate in drinking water (MSG), and 4) a group provided with MSG and HFF (MSG+HFF). Hamsters were euthanized at the end of the 8-month experiment.

Preparation of high-fat diet and monosodium glutamate

The high-fat diet was prepared as previously described [28]. In brief, this diet was prepared by mixing 63.25% of the control diet (Smart Heart, Thailand) with 15% coconut oil, 15% corn oil, 0.5% cholesterol (Sigma-Aldrich, St. Louis, MO, USA), and 0.25% deoxycholate (Sigma-Aldrich), 6% tapioca starch (Fish Band, Thailand). The fat composition of this diet was analyzed by the Central Laboratory, Co. Ltd. (Bangkok, Thailand) (https://www.centrallabthai.com/index.php/th/) using AOAC official methods of analysis. The 10% fructose solution in drinking water was prepared using purified fructose (Merck Millipore, Darmstadt, Germany). Monosodium glutamate was prepared by adding 20 mg/ml of MSG into drinking water (commercial grade, Bangkok, Thailand).

Sample collection and DNA extraction

To avoid bacterial contamination, feces were collected directly from the rectum at the end of the experiment and kept at -20 ˚C until analysis. DNA was extracted from feces using the TIA-Namp Stool DNA kit (Tiangen Biotech, Beijing, China) according to the manufacturer's instructions. The concentration of extracted DNA was measured using a Nanodrop2000 spectrophotometer (NanoDrop Technologies, Wilmington, DE, USA). DNA samples of equal amounts from individual hamsters were pooled by experimental group and kept at -20 ˚C until analysis. Kidney tissue was kept in 10% formalin, followed by processing into paraffin blocks for immunohistochemistry analysis.

Biochemical measurement

The creatinine (Cr) level in serum, a marker commonly used for evaluation of renal function, was measured using enzymatic and colorimetric methods (Cobas 8000 Modular Analysis Series, Roche Diagnostics, Bangkok, Thailand). The data were reported as means ± SD. To compare among different experimental conditions, data were analyzed using analysis of variance (one-way ANOVA) with post-hoc Tukey's HSD (Honestly Significant Difference) test. The analyses were performed using GraphPad Prism version 8.02 (GraphPad Software, La Jolla, CA, USA).

16S rRNA gene sequencing and analysis

A hypervariable region of prokaryotic 16S rRNA (V3-V4 regions) was amplified from fecal DNA by PCR as described previously [29] using a thermal cycler and an Expand high-fidelity PCR system (BioRad C1000TM Thermal Cycler). A quantity of PCR product was

electrophoresed in a 1.5% agarose gel to confirm the size of the product, expected to be about 450–500 bp.

The partial 16S rRNA gene was sequenced using Hiseq2500 (Illumina Inc., California, USA). The 16S sequencing library was prepared by fragmentation of genomic DNA (gDNA) and ligating with specialized adapters to both fragment ends. Paired-end reads were assigned to samples based on their unique barcode and truncated by cutting off the barcode and primer sequences. Paired-end reads which partially overlapped were merged using FLASH (V1.2.7, http://ccb.jhu.edu/software/FLASH/) [30] to produce raw tags. Quality filtering on the raw tags was performed under specific filtering conditions to obtain high-quality clean tags [31] according to the Qiime (V1.7.0, http://qiime.org/scripts/split_libraries_fastq.html) quality-control process. The tags were compared with the reference database (Gold database, http://drive5.com/uchime/uchime_download.html) using the UCHIME algorithm (UCHIME Algorithm, http://www.drive5.com/usearch/manual/uchime_algo.html) [32] to detect chimeric sequences, which were then removed [33]. All tags that successfully passed through these filtering processes were then analyzed using Uparse software (Uparse v7.0.1001 http://drive5.com/uparse/) [34]. Sequences sharing ≥97% similarity were assigned to the same OTU. A representative sequence for each OTU was analyzed for further annotation. Each representative sequence was screened against the SSUrRNA database of the SILVA database (http://www.arb-silva.de/) [35] using Mothur software for annotation at each taxonomic rank (Threshold:0.8~1) [36] (kingdom, phylum, class, order, family and genus). Information on abundance of each OTU was normalized relative to the sample with the fewest sequences. Subsequent analyses of alpha and beta diversity were all performed basing on this normalized data. Alpha diversity indicates species diversity for a sample through two indices, including observed-species and Shannon. We calculated these indices using QIIME (Version 1.7.0) [37] and displayed results using R software (Version 2.15.3) [38]. Beta diversity analysis was used to evaluate differences between samples in species complexity: weighted UniFrac values were calculated using QIIME software (Version 1.7.0) [37].

Sample preparation for NMR analysis

Urine was drawn directly from the urinary bladder using a sterile syringe at the end time point of experiment and kept at -80 ˚C. Samples from each hamster were thawed at room temperature and spun at 18,000 g at 4 ˚C for 10 min. One hundred and eighty μL of the supernatant was thoroughly mixed with 20 μL of 1.5 M potassium phosphate buffer (pH 7.4) containing 100% D_2O, 0.13 mg/mL NaN_3, 1 mg/mL of TSP (3-(trimethylsilyl) propionic-2,2,3,3-d4 acid sodium salt). Finally, 180 μL of the mixture was transferred into a 3 mm NMR tube using an automatic syringe (eVol®) and placed in SampleJet racks (4˚C) until the NMR spectroscopic measurements.

^{1}H NMR data acquisition and statistical analysis

Urine samples were analyzed using a Bruker AVANCE III 600 MHz 1H NMR spectrometer (Bruker; Rheinstetten, Germany), operating at 600.13 MHz at a temperature of 300˚ K using a standard NMR pulse sequence (relaxation delay-90˚-t-90˚-t_m (mixing time)-90˚-acquisition) to acquire one-dimensional spectral data. The parameters used are described elsewhere [39].

^{1}H NMR spectral data were automatically pre-processed (phasing, baseline correction and calibration to TSP) in Topspin 3.6.0. The spectral data were then imported into MATLAB (version R2018a) for statistical analysis. The regions containing water (δ1H 4.70–4.90), urea (δ1H 5.48–6.28) and TSP (δ1H -0.20–0.20) were removed. Alignment was applied using recursive segment-wise peak alignment method [40] and aligned data were normalized using the

probabilistic quotient method prior to multivariate data analyses. Principal component analysis (PCA) and orthogonal projection to latent structures–discriminant analysis (OPLS-DA) were applied to compare ^{1}H NMR spectral data between the different groups. Metabolites that contributed to group discrimination were identified based on a previously published study [41, 42] and confirmed with STOCSY, Chenomx NMR suite 8.3 software (Chenomx Inc. Edmonton, Alberta, Canada) and The Human Metabolome Database (HMDB, http://www. hmdb.ca/).

Histological study

Kidney tissues were fixed in formalin and paraffin-embedded sections were cut at 4 μm thickness, deparaffinized in xylene and rehydrated using a series of graded ethanols (absolute ethanol, 95% alcohol and 70% alcohol) to distilled water. Subsequently, slides were stained with hematoxylin for 10 min and washed in running tap water for 2 min. Slides were destained in acidified alcohol (1% acid in 70% ethanol), rinsed with running tap water and blued in saturated lithium carbonate for 3–4 sec. Then, the slides were rinsed again for 10–20 min before staining with eosin for 15–20 sec, dehydrated and mounted.

Immunohistochemistry

Kidneys from six individuals per experimental group were subjected to immunohistochemistry. Kidney sections (4-μm thickness) were deparaffinized, rehydrated and then antigens retrieved by autoclaving in citrate buffer pH 6.0 for 15 min. Subsequently, endogenous peroxidase activity was blocked by immersing the slides in a solution of 3% hydrogen peroxide in methanol. After blocking with 5% fetal bovine serum (FBS), the sections were incubated with a 1:20 dilution of mouse monoclonal kidney injury molecule-1 (KIM-1) antibody (R&D Systems, Abingdon, UK) and a 1:350 dilution of rabbit polyclonal anti-high mobility group box-1 (HMGB-1) antibody (Abcam, Cambridge, UK) in 1% FBS overnight in a humidified chamber at 4 ˚C. After washing with phosphate buffer saline solution, slides were incubated with a 1:400 dilution of HRP-conjugated sheep anti-mouse IgG (Jackson ImmunoResearch, West Grove, PA, USA) and 1:1000 dilution of HRP-labeled goat anti-rabbit IgG (Jackson ImmunoResearch, West Grove, PA, USA) for 1 h at room temperature. The immunoreactivity signal was generated using diaminobenzidine substrate and counterstained with Mayer's hematoxylin. Localization of immunohistochemical staining was assessed using light microscopy. Brown staining in the cytoplasm of cortical tubules was regarded as indicating the presence of KIM-1. HMGB1 was observed in the nucleus of vascular, proximal and distal tubular cells. Ten fields (200× magnification) of slides stained for both KIM-1 and HMGB-1 were randomly selected for analysis by ImageJ software (National Institutes of Health, Bethesda, MD, USA) [43].

Statistical analysis

The scores for percentage-positive areas of both KIM-1 and HMGB-1 tissues from individual hamsters met the conditions for normality according to a Shapiro-Wilk test. Means of these scores were therefore compared between experimental groups using one-way ANOVA (Analysis of Variance) with a post-hoc Tukey HSD (Honestly Significant Difference) test. A P-value of less than 0.05 was considered to indicate a significant difference between groups. All analyses were performed using SPSS version 26.0 (IBM, Armonk, NY, USA) and GraphPad Prism version 8.02 (GraphPad Software, La Jolla, CA, USA).

Results

A combination of MSG and HFF diets exacerbates kidney pathology without affecting serum creatinine levels

In the histological study by H&E (Fig 1A), the normal control hamsters showed normal tubular cells and glomeruli, while mild, moderate and severe renal tubular dilatation were found in hamsters treated with MSG, HFF and MGS+HFF, respectively. Next, we sought to evaluate renal function by measurement of creatinine level in serum. This level, in all experimental groups, was within the reference range for hamsters (0.4–1.0 mg/dL) [44] and did not statistically differ among groups ($p > 0.05$) as shown in Fig 1B.

A combination of MSG and HFF diets increases KIM-1 and HMGB-1 expression in renal tissue

Base on histopathological demonstration on stained slides, we evaluated location and expression levels of KIM-1 and HMGB-1, renal injury markers, using immunohistochemistry (Fig 1). Expression of KIM-1 was observed mainly in the cortex on the apical side of proximal tubules. KIM-1-positive cells were observed in membranes and cytoplasm of proximal tubular cells with some regional differences within tubules. In comparison to normal control hamsters, the percentage of the positive area of KIM-1 was statistically significantly higher in all groups fed with a modified diet: MSG ($p < 0.05$), HFF ($p < 0.005$) and MSG+HFF ($p < 0.0001$) (Fig 1C). However, the expression levels of KIM-1 and HMGB-1 between the MSG and HFF groups were not statistically different (Fig 1C and 1D). Expression of both marker molecules was significantly higher in the MSG+HFF group than in all other groups (Fig 1C and 1D).
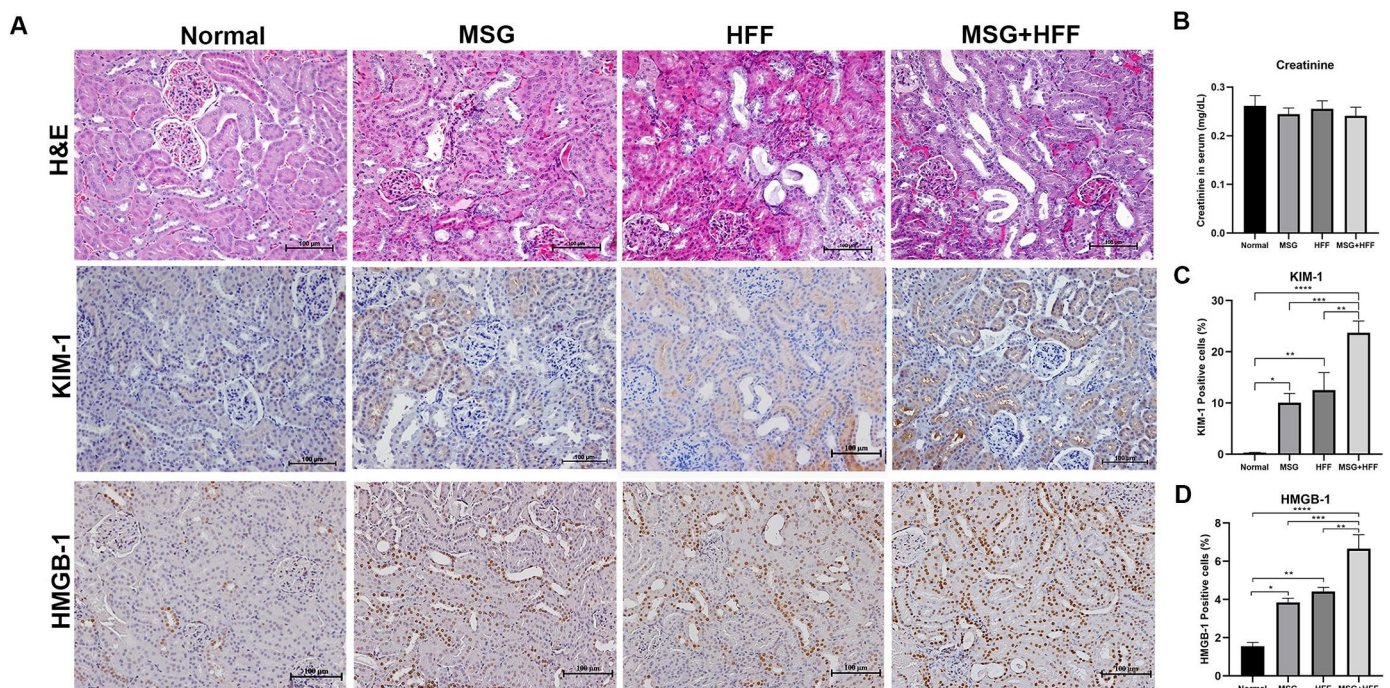
Fig 1. (A) Representative photographs of sections of hamster kidneys stained by H&E and for expression of kidney injury molecule-1 (KIM-1) and high-mobility group box 1 protein (HMGB1), (B) serum creatinine levels and percentages of (C) KIM-1- and (D) HMGB1-positive cells. The extent of injury in these kidneys was evaluated after 8 months on experimental diets including the normal group (n = 6), monosodium glutamate-treated group (MSG, n = 6), high-fat and high-fructose diet-treated group (HFF, n = 6) and the MSG and HFF diet-treated group (MSG+HFF, n = 6). Findings are presented as mean ± SEM. *, **, *** are $p < 0.05$, $p < 0.01$ and $p < 0.0001$, respectively, compared with normal control or MSG or HFF.

A combination diet of MSG and HFF changes the gut microbiota composition

Fifteen microbial phyla, 28 classes, 39 orders, 65 families and 150 genera were detected across all samples. To show the relative abundance of bacterial communities more intuitively, we selected the top 10 species identified in each sample or group and generated percentage stacked histograms of relative abundance at phylum, class, order, family and genus levels (Fig 2).

At the phylum level (Fig 2A), Bacteroidetes, Firmicutes and Proteobacteria were abundant in all experimental groups. The abundance of Euryarchaeota was higher in groups fed modified diets; 5.94% for HFF, 11.17% for MSG, and 17.32% for the MSG+HFF group, while this phylum constituted only 0.05% of reads in the normal control group. Notably, Bacteroidetes slightly decreased from 55.99% in the normal control to 55.06% in HFF, 52.98% in the MSG group and to 42.32% in the MSG+HFF group. Likewise, the abundance of Firmicutes decreased from 28.63% in the normal control group to 22.71% in the MSG group. The ratio of Firmicutes/Bacteroidetes was higher in the MSG+HFF group (0.675) compared to either MSG (0.429), HFF (0.519) or normal control (0.511) groups.

At the class level (Fig 2B), the relative abundance of the top 4 bacterial classes was observed in the order Bacteroidia > Clostridia > Deltaproteobacteria > Unidentified_Saccharibacteria in all experimental groups. Methanobacteria was observed only in groups fed the modified diets. The relative abundance of Bacteroidia showed a decreasing trend from 55.99% in the normal control group to 55.06% in HFF, 52.98% in MSG and 42.32% in the MSG+HFF groups. On the other hand, the proportion of Methanobacteria increased from 0.05% in the normal control group to 5.92% in HFF, 11.17% in MSG and 17.32% in the MSG+HFF group. Notably, abundance of reads from Methanobacteria in the MSG+HFF group was 346.40-fold higher than in the normal control group, 118.4-fold higher than in the MSG group and 223.4-fold more than in the HFF group.

At the order level (Fig 2C), the most abundant taxa were observed in the following order in all experimental groups: Bacteroidales > Clostridiales > Desulfovibrionales > Unidentified_Saccharibacteria. Methanobacteriales was observed only in groups fed a modified diet. Notably, in the MSG+HFF groups, Bacteroidia was least abundant and Methanobacteria was most abundant. Abundance of Desulfovibrionales decreased from 8.32% in the normal control group to 5.96% in MSG, 4.92% in HFF and 4.89% in the MSG+HFF group.

The four most abundant families (Fig 2D) were observed in all experimental groups in the following order: Bacteroidales_S24-7_group > Ruminococcaceae > Desulfovibrionaceae > Lachnospiraceae. The MSG+HFF group had the lowest level of Bacteroidales_S24-7_group, Desulfovibrionaceae and Erysipelotrichaceae, but the highest abundance of Eubacteriaceae and Methanobacteriaceae.

As shown in Fig 2E, the top four gut bacterial genera found in all experimental groups were *Desulfovibrio* (MN326533), *Ruminococcaceae*_UCG-014 (MN326541), and the [*Eubacterium*] _coprostanoligenes_group (MN326531). In the MSG+HFF group, *Methanobrevibacter* (MN326530), *Lachnospiraceae*_NK4A136_group (MN326551) and *Escherichia-Shigella* (MN326536) were more abundant than in the other groups, while *Lactobacillus* (MN326537), *Desulfovibrio* (MN326533), *Ruminococcaceae*_UCG-014 (MN326541) and *Allobaculum* (MN326542) were less abundant.

A heatmap of the top 35 genera observed in all groups is shown in Fig 3. Relative to the normal control group, *Citrobacter* (MN326558), *Roseburia* (MN326554) and *Ruminococcus*_1 (MN326532) were found to have the highest level in the MSG treated group. Similarly, *Citrobacter* (MN326558) was 58-fold more abundant in the MSG group. In the HFF group, *Dorea*
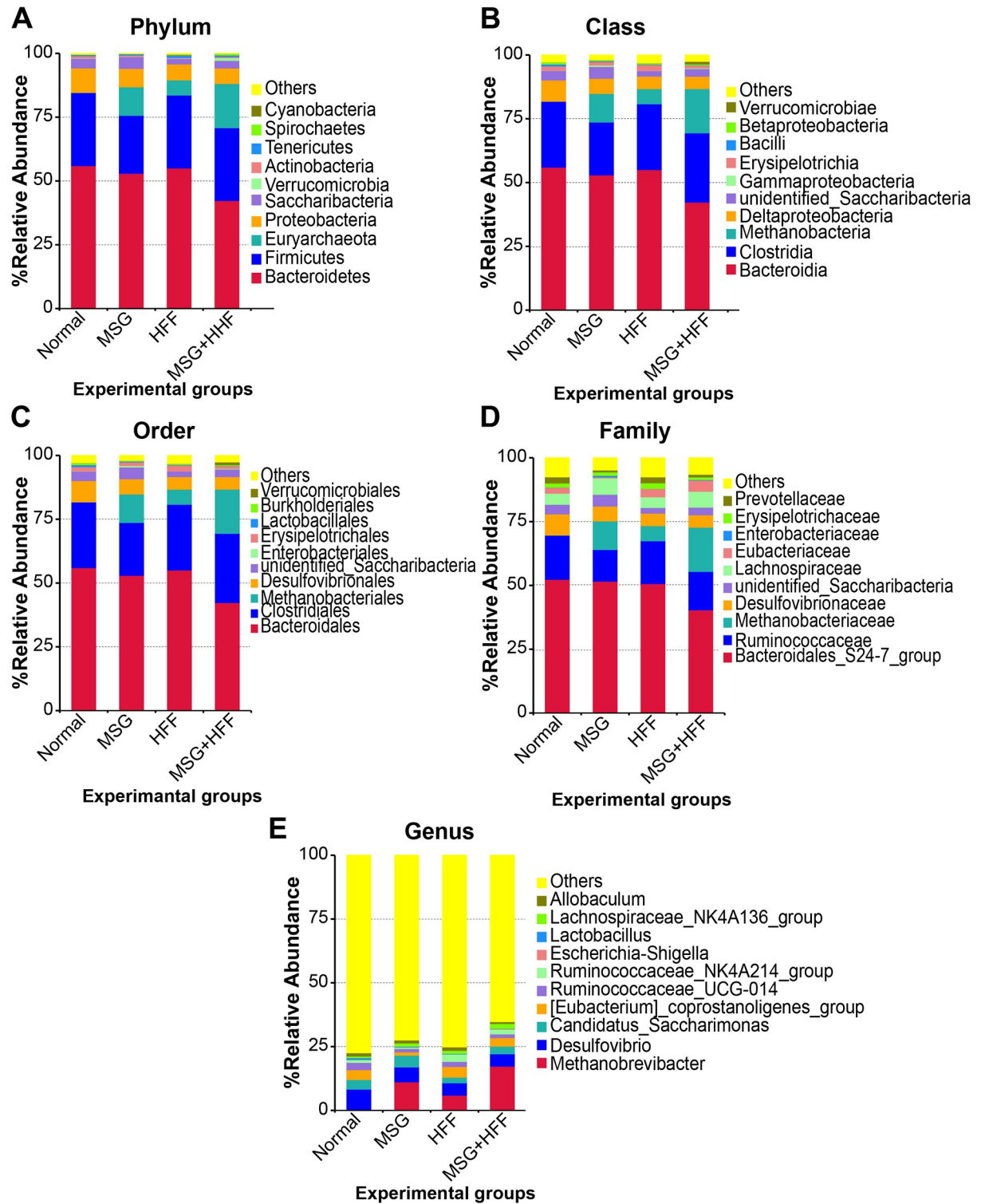
Fig 2. Fecal microbial composition in hamsters at different taxonomic levels. The columns represent a normal group (n = 10), monosodium glutamate-treated group (MSG) (n = 10), high-fat and high-fructose diet-treated (HFF) (n = 10) and MSG and HFF diet-treated (MSG+HFF) (n = 10).
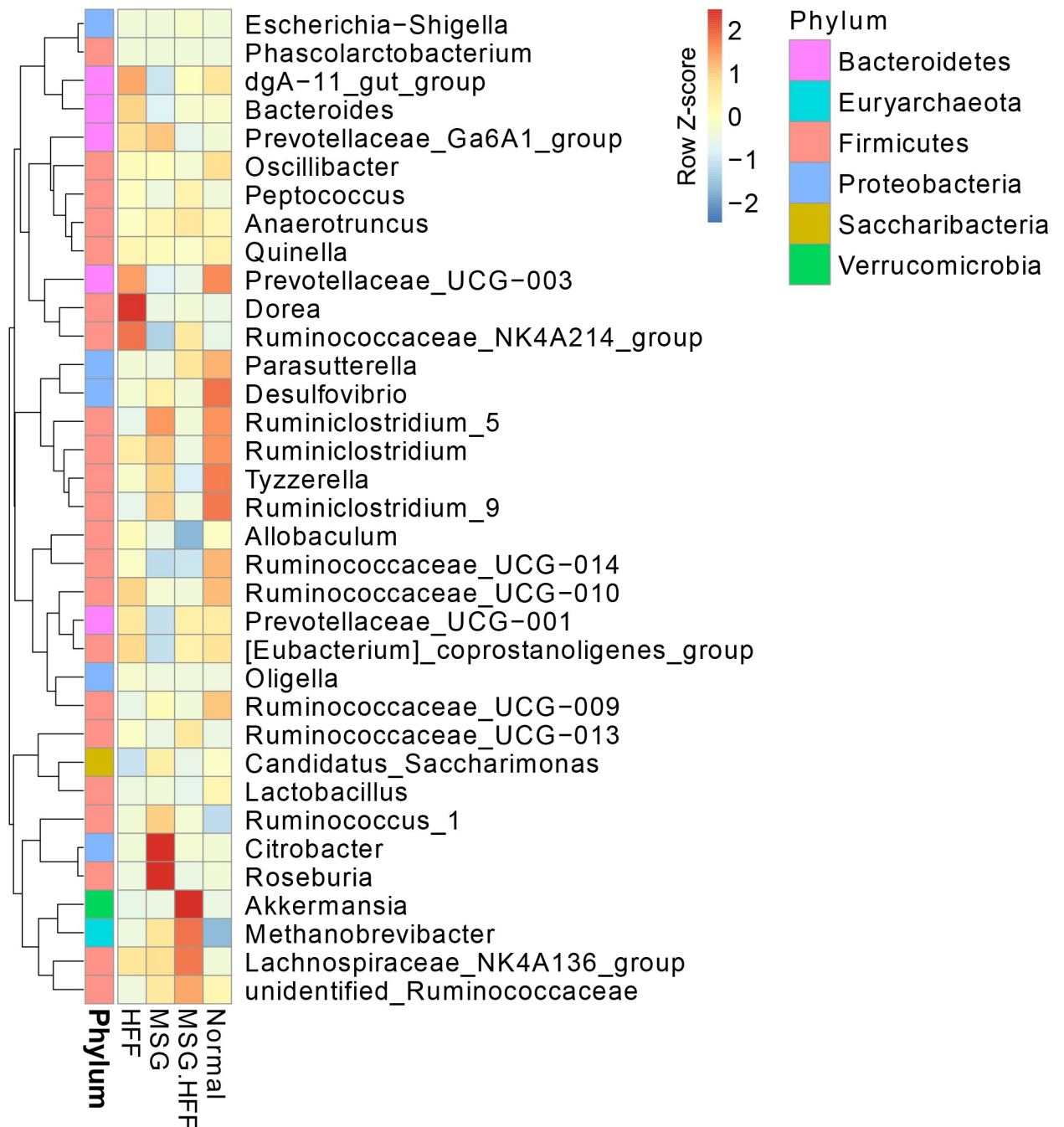
Fig 3. Composition of the gut microbiota. Heat map of the top 35 bacterial genera identified from hamster fecal DNA. The abundances were arranged using unsupervised hierarchical cluster analysis (blue, low abundance; red, high abundance).

https://doi.org/10.1371/journal.pone.0231237.g003

(MN326559), *Ruminococcaceae*_NK4A214_group (MN326535), dgA-11_gut_group (MN326549), *Desulfovibrio* (MN326533), *Bacteroides* (MN326550) and *Oligella* (MN326546) were present in greatly increased abundance. In addition, *Methanobrevibacter* (MN326530), *Akkermansia* (MN326539), *Escherichia-Shigella* (MN326536), *Lachnospiraceae*_N-K4A136_group (MN326551), unidentified_*Ruminococcaceae* (MN326547), *Anaerotruncus*

(MN326560), *Peptococcus* (MN326556) were highly elevated (relative to the normal control group) in the MSG+HFF group by 372.54, 13.15, 3.42, 3.19, 1.40, 1.15 and 1.81-fold, respectively. In contrast, *Lactobacillus* (MN326537), *Tyzzerella* (MN326538), *Ruminiclostridium* (MN326563), *Allobaculum* (MN326542), *Prevotellaceae*_Ga6A1_group (MN326553) and *Quinella* (MN326546) were less abundant by 6.74, 3.76, 2.17, 1.75, 1.33 and 1.28-fold, respectively, in the MSG+HFF group when compared to the normal group. Interestingly, in the MSG+HFF group, the genera *Akkermansia* (MN326539) and *Escherichia-Shigella* (MN326536) were 14.10- and 3.90-fold, respectively, more abundant than in the MSG group and 15.18- and 8.70-fold, respectively, more abundant than in the HFF group.

Fig 4 shows alpha and beta gut microbial diversity. Alpha diversity did not differ among the normal, MSG and HFF groups but was lower in the MSG+HFF group (Fig 4A and 4B). The weighted UniFrac distance cluster analysis (UPGMA) was used to show the similarity between the different experimental groups. The bacterial communities were more similar in the normal control, MSG and HFF groups relative to the MGS+HFF group (Fig 4C).

## A combination of MSG and HFF diets changes urine metabolite levels

^{1}H NMR spectroscopy was used to obtain urine metabolite profiles from each group of hamsters (S1 Fig). Three metabolites, trimethylamine *N*-oxide (TMAO), indoxyl sulfate and *p*-cresol sulfate involved in metabolite-related kidney injury, were selected for presentation in Table 1.

The level of TMAO was significantly lower in urine from the MSG+HFF group ($p < 0.05$) when compared to the normal control and MSG groups. Levels of indoxyl sulfate were also significantly lower in the HFF group ($p < 0.001$) and the MSG+HFF group ($p < 0.01$) compared to the normal control and MSG groups. In contrast, compared to normal controls, the level of *p*-cresol sulfate was significantly higher in the HFF group ($p < 0.001$) and in the MSG+HFF group ($p < 0.05$), but was lower in the MSG group. Likewise, levels of this urine metabolite were significantly higher in the HFF group ($p < 0.001$) and the MSG+HFF group ($p < 0.05$) when compared with the MSG group alone.

Discussion

Alteration of gut microbiota composition results in a change in gut-derived metabolites, some of which are uremic toxins that can induce renal damage [45, 46]. Here, we have reported the effects of MSG in combination with HFF diets on kidney injury and co-observation of gut dysbiosis and urine metabolite alteration in hamsters. The MSG dose (20 mg/ml) was used based on an average MSG intake in humans (0.4–14 gm/day) [12]. A combination of MSG and HFF diets led to greater damage to kidney tissues, alteration of the gut microbiota, decrease in urine trimethylamine *N*- oxide (TMAO) and indoxyl sulfate and increase of *p*-cresol sulfate production relative to animals fed MSG or HFF alone. Increased levels of blood uremic toxins such as *p*-cresol sulfate might cause kidney damage in our animal model as reflected by the greater amount of this metabolite in urine. A postulated mechanism of kidney injury is summarized in Fig 5.

It is well known that consumption of MSG or a HFF diet has the potential to induce kidney injury, reflected in changing histology in kidney tissues [47–49]; however, there is no information on the effect of these in combination on kidney pathology. Here we present such information for the first time. We found that an MSG+HFF diet exacerbated kidney injury, such as tubular dilatation, more than did a single diet type. One unexpected result was that serum creatinine did not deviate from normal controls, suggesting that any injury to kidney tissue in this model must be at an early stage. That some injury occurring was supported by the high
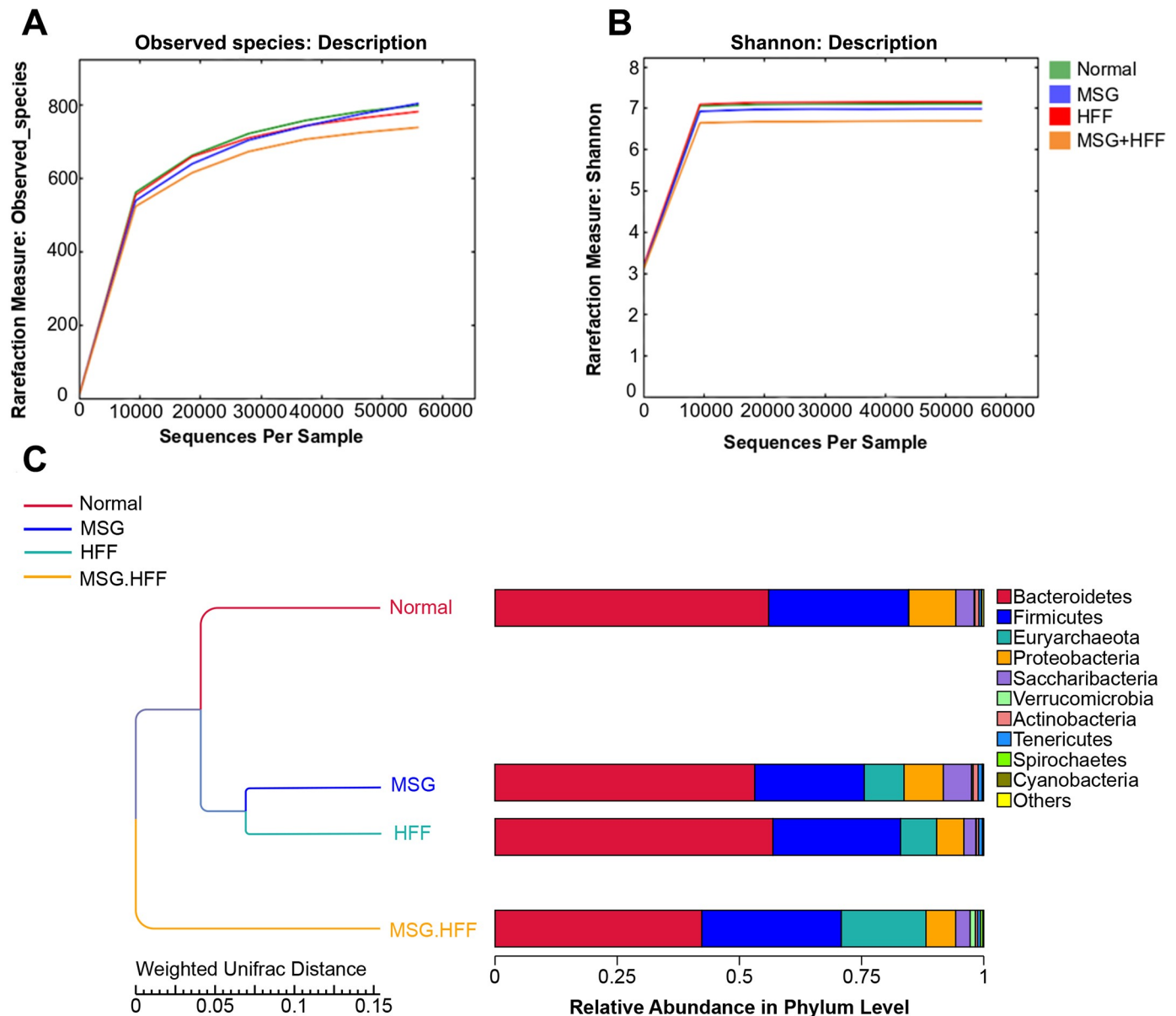
Fig 4. Alpha diversity of the sequence reads from DNA extracted from hamster feces for each group. (A) rarefaction analysis of the observed taxa and (B) the Shannon index. (C) Beta diversity, UPMGA clustering trees-weighted Unifrac distance. The results of clustering using two distance matrixes were combined with the overall percentages of relative abundance among all samples at phylum level.

expression levels of the renal injury markers, KIM-1 and HMGB-1 [50, 51]. These markers might prove useful for diagnosis of early kidney damage.

Many reviews have revealed that alteration of gut microbiota plays an important role in causing kidney injury [14, 27, 52]. Hence, we further verified the effect of this change in our animal model. Sequencing of prokaryotic 16S rRNA sequences (V3-V4 regions) revealed that the MSG+HFF diet can reshape composition of gut microbiota. Hamsters fed on this diet had much lower abundance of Bacteroidetes, but increased Euryarchaeota at phylum, class, order, family and genus levels relative to animals fed either diet alone. This finding was supported by the high ratio of Firmicutes/ Bacteroidetes in the MSG+HFF group, in agreement with

Table 1. Pairwise comparisons of differentially produced urine metabolites among experimental groups.

Metabolites	N/MSG	N/HFF	N/MSG+HFF	MSG/HFF	MSG/MSG+HFF	HFF/MSG+HFF
TMAO	↑	↑	↓***	↓*	↓*	↓
Indoxyl sulfate	↑	↓***	↓**	↓***	↓**	↑
p-cresol sulfate	↓	↑***	↑*	↑***	↑*	↓*

Arrows represent any metabolic changes, associated with specific diets in hamster urine in pairwise comparisons among experimental groups. Significant differences are indicated by *, **, and *** which correspond to $p < 0.05$, < 0.01, and < 0.001, respectively. TMAO; trimethylamine N-oxide, N; Normal; MSG, monosodium glutamate-treated group; HFF, high-fat and high-fructose diet-treated; MSG+HFF, group receiving a diet containing both MSG and HFF.

findings of Feng *et al*. [53]. Alpha diversity and weighted Unifrac distance cluster analysis at the phylum level distinguished bacterial populations in animals fed with the combined diet from those given a single diet. In hamsters treated with MSG alone, changes in the gut microbiota were relatively slight, agreeing with a previous report in humans [18]. MSG led to increases in *Roseburia* (MN326554), *Citrobacter* (MN326558) and *Ruminococcus*_1 (MN326532). Increase of *Roseburia* after MSG consumption has been reported previously [18]. *Roseburia* is a taxon of anaerobic gut bacteria associated with butyrate production and
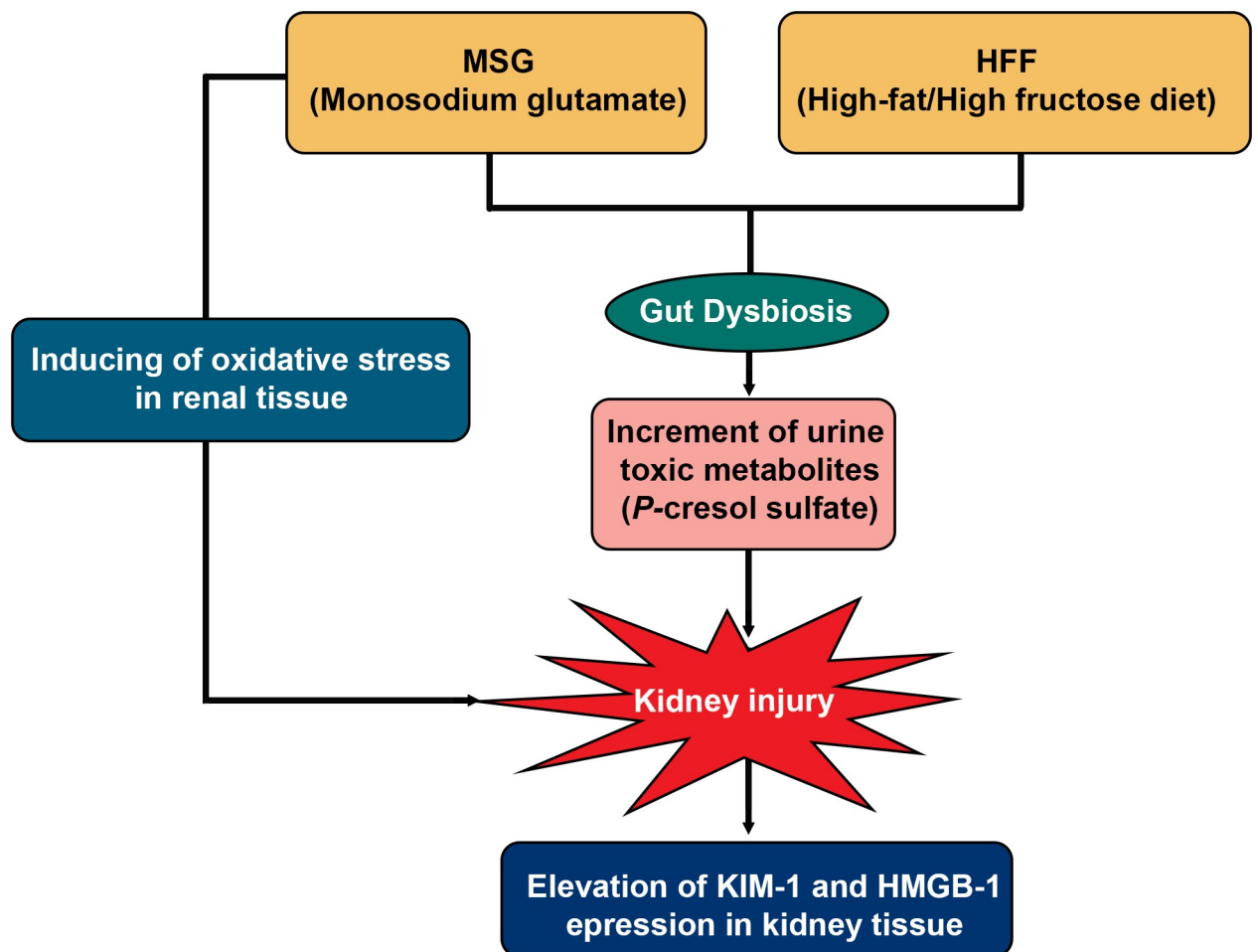
Fig 5. Postulated mechanism by which the MSG+HFF diet might cause kidney injury.

negatively related to CKD progression [19, 55]. However, the increment of *Roseburia* (MN326554) level in this study might be due to MSG intake because glutamate in MSG can convert to butyrate [19, 54, 55]. The genus *Citrobacter* (Family Enterobacteriaceae) can produce the enzyme tyrosine phenol-lyase for converting L-tyrosine to 4-hydroxyphenylpyruvate and 4-hydroxyphenylpyruvate be further metabolized into *p*-cresol sulfate in the liver [56, 57]. In hamsters fed the HFF diet, an increase of *Dorea*, *Ruminococcaceae*_NK4A214_group (MN326535), dgA-11_gut_group (MN326549), *Desulfovibrio* (MN326533), *Bacteroides* (MN326550) and *Oligella* (MN326548) was found, similar to previous studies [58, 59]. *Desulfovibrio* (Family Desulfovibrionaceae) produces urea. An increment of urea level indicates kidney damage [54, 60]. Elevation of *Desulfovibrio* may thus serve as a microbiomarker for kidney injury. However, in relation to the MSG+HFF diet, a previous study in growing pigs found that dietary supplementation with fat and MSG increases the *Clostridium coccoides* group, *Fusobacterium prausnitzii*, *Peptostreptococcus productus*, *Faecalibacterium prausnitzii*, *Prevotella* and *Roseburia* in the cecum, but decreases *Bacteroides thetaiotaomicron* and the *Clostridium leptum* subgroup [53]. These differences might be explained by the different animal models used [61] and different diet compositions [62].

Among the changes in gut microbiota, we found an increase of *Methanobrevibacter* (MN326530) in the HFF+MSG group. This genus is an archaeon in the phylum Euryarchaeota. An increase in abundance of *Methanobrevibacter* may be associated with obesity [63] and kidney injury [64]. *Methanobrevibacter* promotes fermentation of polysaccharides by removal of H_2, resulting in an increase in levels of short-chain fatty acids in the colon and host adiposity [54]. Elevated representation of *Methanobrevibacter* is also found in rats fed with a high-fat diet [65]. In addition, levels of beneficial bacterial genera such as *Lactobacillus* (MN326537) and *Allobaculum* (MN326542) [66] were lower in hamsters exposed to either MSG or HFF diets. *Lactobacillus* can be an antioxidant and reduce uremic toxins in serum [67, 68]. A decrease in *Lactobacillus* abundance might affect the level of uremic toxin. The lowest proportion of these beneficial bacteria was found in hamsters fed on the MSG+HFF diet, consistent with results from previous reports [20, 69]. In contrast, relative abundance of pathogenic bacteria, such as members of the *Escherichia-Shigella* (MN326536) genus, increased in hamsters given the MSG and/or the HFF diet. The highest abundance of this genus was seen in the MSG +HFF group, similar to the result from a previous report [70]. Taken together, the bacterial composition, Firmicutes/ Bacteroidetes ratio, as well as alpha and beta diversity indicate that the MSG+HFF diet increases gut dysbiosis in hamsters more than does either diet alone.

Gut dysbiosis causes alteration of gut-derived metabolites including TMAO, indoxyl sulfate and *p*-cresol sulfate, which are uremic toxins that contribute to kidney injury [45, 52, 71–74]. We found that a combination of MSG and HFF led to increased *p*-cresol sulfate level but decreased TMAO and indoxyl sulfate levels in urine compared to normal controls. *P*-cresol sulfate, a major component of urinary myelin basic protein-like material, causes renal tubular cell damage by inducing oxidative stress [74]. As noted above, we found that the highest relative abundance of *Akkermansia* (MN326539) and an increase in *p*-cresol sulfate levels were seen in the MSG+HFF group. The association between *Akkermansia* and *p*-cresol sulfate metabolite has been recently reviewed [75].

TMAO is another important gut-derived metabolite contributing to kidney injury by promoting renal functional impairment and regulating the profibrotic transforming growth factor-β(TGF-beta)/Smad3 signaling pathway [73]. Hamsters fed with a combination of MSG and the HFF diet had decreased TMAO levels in urine, but an increase of *Methanobrevibacter* (MN326530) in the feces. An association between *Methanobrevibacter* and a reduction of TMAO plasma metabolite has been reported previously [76]. Possibly, the reduction of TMAO level that was observed in urine might be due to activities of other gut microbiota. In

contrast, mice fed with a high-fat diet for 16 weeks to induce obesity exhibited elevated circulating levels of TMAO, resulting in renal interstitial fibrosis and dysfunction [73]. The different findings suggest that ingredients of diets, duration of exposure and species of animal used can all affect gut dysbiosis and host-microbial co-metabolism. Taken together, these changes could contribute to cause kidney injury [46, 52, 73]

Conclusions

A combination of MSG and HFF diets increased severity of kidney injury and altered gut microbiota and urine metabolites much more than did either diet alone. Our findings should raise awareness about the important role of MSG and HFF diets in development of human kidney disease and might indicate intervention strategies that could be used to limit kidney disease.

Supporting information

S1 Fig. Representative of ^{1}H nuclear magnetic resonance (NMR) spectra of urine samples obtained from a normal control (A), monosodium glutamate-treated (MSG) individual (B), high-fat and high-fructose diet-treated (HFF) individual (C); and a hamster given the MSG and HFF diet (MSG+HFF) (D). 3-IS = 3-indoxyl sulfate; P-CS = *p*-cresol sulfate; TMAO = trimethylamine *N*-oxide.
(TIF)

Acknowledgments

Author Contributions

Writing – original draft: Thatsanapong Pongking, Kitti Intuyod.

Writing – review & editing: Somchai Pinlaor, Porntip Pinlaor.

References

1. Popkin BM, Adair LS, Ng SW. Global nutrition transition and the pandemic of obesity in developing countries. Nutr Rev. 2012; 70(1):3–21. Epub 2012/01/10. https://doi.org/10.1111/j.1753-4887.2011.00456.x PMID: 22221213.

2. Popkin BM. Nutrition Transition and the Global Diabetes Epidemic. Curr Diab Rep. 2015; 15(9):64. Epub 2015/07/27. https://doi.org/10.1007/s11892-015-0631-4 PMID: 26209940.

3. Hill NR, Fatoba ST, Oke JL, Hirst JA, O'Callaghan CA, Lasserson DS, et al. Global Prevalence of Chronic Kidney Disease—A Systematic Review and Meta-Analysis. PLoS One. 2016; 11(7):e0158765. Epub 2016/07/08. https://doi.org/10.1371/journal.pone.0158765 PMID: 27383068.

4. Jha V, Garcia-Garcia G, Iseki K, Li Z, Naicker S, Plattner B, et al. Chronic kidney disease: global dimension and perspectives. Lancet. 2013; 382(9888):260–72. Epub 2013/06/04. https://doi.org/10.1016/S0140-6736(13)60687-X PMID: 23727169.

5. Ingsathit A, Thakkinstian A, Chaiprasert A, Sangthawan P, Gojaseni P, Kiattisunthorn K, et al. Prevalence and risk factors of chronic kidney disease in the Thai adult population: Thai SEEK study. Nephrol Dial Transplant. 2010; 25(5):1567–75. Epub 2009/12/29. https://doi.org/10.1093/ndt/gfp669 PMID: 20037182.

6. Gentile CL, Weir TL. The gut microbiota at the intersection of diet and human health. Science. 2018; 362(6416):776–80. Epub 2018/11/18. https://doi.org/10.1126/science.aau5812 PMID: 30442802.

7. Asghari G, Momenan M, Yuzbashian E, Mirmiran P, Azizi F. Dietary pattern and incidence of chronic kidney disease among adults: a population-based study. Nutr Metab (Lond). 2018; 15(1):88. Epub 2018/12/20. https://doi.org/10.1186/s12986-018-0322-7 PMID: 30564279.

8. Ortiz GG, Bitzer-Quintero OK, Zarate CB, Rodriguez-Reynoso S, Larios-Arceo F, Velazquez-Brizuela IE, et al. Monosodium glutamate-induced damage in liver and kidney: a morphological and biochemical approach. Biomed Pharmacother. 2006; 60(2):86–91. Epub 2006/02/21. https://doi.org/10.1016/j.biopha.2005.07.012 PMID: 16488110.

9. Sharma A. Monosodium glutamate-induced oxidative kidney damage and possible mechanisms: a mini-review. J Biomed Sci. 2015; 22:93. Epub 2015/10/27. https://doi.org/10.1186/s12929-015-0192-5 PMID: 26493866.

10. Sharma A, Prasongwattana V, Cha'on U, Selmi C, Hipkaeo W, Boonnate P, et al. Monosodium glutamate (MSG) consumption is associated with urolithiasis and urinary tract obstruction in rats. PLoS One. 2013; 8(9):e75546. Epub 2013/10/03. https://doi.org/10.1371/journal.pone.0075546 PMID: 24086562.

11. Paul MV, Abhilash M, Varghese MV, Alex M, Nair RH. Protective effects of alpha- tocopherol against oxidative stress related to nephrotoxicity by monosodium glutamate in rats. Toxicol Mech Methods. 2012; 22(8):625–30. Epub 2012/07/26. https://doi.org/10.3109/15376516.2012.714008 PMID: 22827614.

12. Insawang T, Selmi C, Cha'on U, Pethlert S, Yongvanit P, Areejitranusorn P, et al. Monosodium glutamate (MSG) intake is associated with the prevalence of metabolic syndrome in a rural Thai population. Nutr Metab (Lond). 2012; 9(1):50. Epub 2012/06/12. https://doi.org/10.1186/1743-7075-9-50 PMID: 22681873.

13. Weerawatanakorn M. Dicarbonyl compounds and sugar contents of Thai commercial beverages. Songklanakarin Journal of Science & Technology. 2013; 35(6).

14. Sekirov I, Russell SL, Antunes LC, Finlay BB. Gut microbiota in health and disease. Physiol Rev. 2010; 90(3):859–904. Epub 2010/07/29. https://doi.org/10.1152/physrev.00045.2009 PMID: 20664075.

15. Cerda B, Perez M, Perez-Santiago JD, Tornero-Aguilera JF, Gonzalez-Soltero R, Larrosa M. Gut Microbiota Modification: Another Piece in the Puzzle of the Benefits of Physical Exercise in Health? Front Physiol. 2016; 7:51. Epub 2016/03/01. https://doi.org/10.3389/fphys.2016.00051 PMID: 26924990

16. Hawrelak JA, Myers SP. The causes of intestinal dysbiosis: a review. Altern Med Rev. 2004; 9(2):180–97. Epub 2004/07/16. PMID: 15253677.

17. DuPont AW, DuPont HL. The intestinal microbiota and chronic disorders of the gut. Nat Rev Gastroenterol Hepatol. 2011; 8(9):523–31. Epub 2011/08/17. https://doi.org/10.1038/nrgastro.2011.133 PMID: 21844910.

18. Peng QN, Huo DX, Ma CC, Jiang SM, Wang LS, Zhang JC. Monosodium glutamate induces limited modulation in gut microbiota. Journal of Functional Foods. 2018; 49:493–500. https://doi.org/10.1016/j.jff.2018.09.015

19. Jiang S, Xie S, Lv D, Zhang Y, Deng J, Zeng L, et al. A reduction in the butyrate producing species *Roseburia* spp. and *Faecalibacterium prausnitzii* is associated with chronic kidney disease progression.

Antonie Van Leeuwenhoek. 2016; 109(10):1389–96. Epub 2016/07/20. https://doi.org/10.1007/s10482-016-0737-y PMID: 27431681.

20. Do MH, Lee E, Oh MJ, Kim Y, Park HY. High-Glucose or -Fructose Diet Cause Changes of the Gut Microbiota and Metabolic Disorders in Mice without Body Weight Change. Nutrients. 2018; 10(6). Epub 2018/06/15. https://doi.org/10.3390/nu10060761 PMID: 29899272

21. Murphy EA, Velazquez KT, Herbert KM. Influence of high-fat diet on gut microbiota: a driving force for chronic disease risk. Curr Opin Clin Nutr Metab Care. 2015; 18(5):515–20. Epub 2015/07/15. https://doi.org/10.1097/MCO.0000000000000209 PMID: 26154278

22. Altunkaynak ME, Ozbek E, Altunkaynak BZ, Can I, Unal D, Unal B. The effects of high- fat diet on the renal structure and morphometric parametric of kidneys in rats. J Anat. 2008; 212(6):845–52. Epub 2008/05/31. https://doi.org/10.1111/j.1469-7580.2008.00902.x PMID: 18510511

23. Rosas-Villegas A, Sanchez-Tapia M, Avila-Nava A, Ramirez V, Tovar AR, Torres N. Differential Effect of Sucrose and Fructose in Combination with a High Fat Diet on Intestinal Microbiota and Kidney Oxidative Stress. Nutrients. 2017; 9(4). Epub 2017/04/20. https://doi.org/10.3390/nu9040393 PMID: 28420148

24. Xu KY, Xia GH, Lu JQ, Chen MX, Zhen X, Wang S, et al. Impaired renal function and dysbiosis of gut microbiota contribute to increased trimethylamine-N-oxide in chronic kidney disease patients. Sci Rep. 2017; 7(1):1445. Epub 2017/05/05. https://doi.org/10.1038/s41598-017-01387-y PMID: 28469156

25. Evenepoel P, Glorieux G, Meijers B. p-cresol sulfate and indoxyl sulfate: some clouds are gathering in the uremic toxin sky. Kidney Int. 2017; 92(6):1323–4. Epub 2017/11/21. https://doi.org/10.1016/j.kint.2017.06.029 PMID: 29153138.

26. Shafi T, Sirich TL, Meyer TW, Hostetter TH, Plummer NS, Hwang S, et al. Results of the HEMO Study suggest that p-cresol sulfate and indoxyl sulfate are not associated with cardiovascular outcomes. Kidney Int. 2017; 92(6):1484–92. Epub 2017/07/26. https://doi.org/10.1016/j.kint.2017.05.012 PMID: 28739139

27. Aron-Wisnewsky J, Clement K. The gut microbiome, diet, and links to cardiometabolic and chronic disorders. Nat Rev Nephrol. 2016; 12(3):169–81. Epub 2015/12/01. https://doi.org/10.1038/nrneph.2015.191 PMID: 26616538.

28. Chaidee A, Onsurathum S, Intuyod K, Haonon O, Pannangpetch P, Pongchaiyakul C, et al. Opisthorchis viverrini Infection Augments the Severity of Nonalcoholic Fatty Liver Disease in High-Fat/High-Fructose Diet-Fed Hamsters. Am J Trop Med Hyg. 2019. Epub 2019/09/05. https://doi.org/10.4269/ajtmh.19-0442 PMID: 31482785.

29. Itthitaetrakool U, Pinlaor P, Pinlaor S, Chomvarin C, Dangtakot R, Chaidee A, et al. Chronic Opisthorchis viverrini Infection Changes the Liver Microbiome and Promotes Helicobacter Growth. PLoS One. 2016; 11(11):e0165798. Epub 2016/11/03. https://doi.org/10.1371/journal.pone.0165798 PMID: 27806126

30. Magoc T, Salzberg SL. FLASH: fast length adjustment of short reads to improve genome assemblies. Bioinformatics. 2011; 27(21):2957–63. Epub 2011/09/10. https://doi.org/10.1093/bioinformatics/btr507 PMID: 21903629

31. Bokulich NA, Subramanian S, Faith JJ, Gevers D, Gordon JI, Knight R, et al. Quality- filtering vastly improves diversity estimates from Illumina amplicon sequencing. Nat Methods. 2013; 10(1):57–9. Epub 2012/12/04. https://doi.org/10.1038/nmeth.2276 PMID: 23202435

32. Edgar RC, Haas BJ, Clemente JC, Quince C, Knight R. UCHIME improves sensitivity and speed of chimera detection. Bioinformatics. 2011; 27(16):2194–200. Epub 2011/06/28. https://doi.org/10.1093/bioinformatics/btr381 PMID: 21700674

33. Haas BJ, Gevers D, Earl AM, Feldgarden M, Ward DV, Giannoukos G, et al. Chimeric 16S rRNA sequence formation and detection in Sanger and 454-pyrosequenced PCR amplicons. Genome Res. 2011; 21(3):494–504. Epub 2011/01/08. https://doi.org/10.1101/gr.112730.110 PMID: 21212162

34. Edgar RC. UPARSE: highly accurate OTU sequences from microbial amplicon reads. Nat Methods. 2013; 10(10):996–8. Epub 2013/08/21. https://doi.org/10.1038/nmeth.2604 PMID: 23955772.

35. Wang Q, Garrity GM, Tiedje JM, Cole JR. Naive Bayesian classifier for rapid assignment of rRNA sequences into the new bacterial taxonomy. Appl Environ Microbiol. 2007; 73(16):5261–7. Epub 2007/06/26. https://doi.org/10.1128/AEM.00062-07 PMID: 17586664

36. Quast C, Pruesse E, Yilmaz P, Gerken J, Schweer T, Yarza P, et al. The SILVA ribosomal RNA gene database project: improved data processing and web-based tools. Nucleic Acids Res. 2013; 41(Database issue):D590–6. Epub 2012/11/30. https://doi.org/10.1093/nar/gks1219 PMID: 23193283

37. Caporaso JG, Kuczynski J, Stombaugh J, Bittinger K, Bushman FD, Costello EK, et al. QIIME allows analysis of high-throughput community sequencing data. Nat Methods. 2010; 7(5):335–6. Epub 2010/04/13. https://doi.org/10.1038/nmeth.f.303 PMID: 20383131

38. White JR, Nagarajan N, Pop M. Statistical methods for detecting differentially abundant features in clinical metagenomic samples. PLoS Comput Biol. 2009; 5(4):e1000352. Epub 2009/04/11. https://doi.org/10.1371/journal.pcbi.1000352 PMID: 19360128

39. Beckonert O, Coen M, Keun HC, Wang Y, Ebbels TM, Holmes E, et al. High-resolution magic-angle-spinning NMR spectroscopy for metabolic profiling of intact tissues. Nat Protoc. 2010; 5(6):1019–32. Epub 2010/06/12. https://doi.org/10.1038/nprot.2010.45 PMID: 20539278.

40. Veselkov KA, Lindon JC, Ebbels TM, Crockford D, Volynkin VV, Holmes E, et al. Recursive segment-wise peak alignment of biological (1)H NMR spectra for improved metabolic biomarker recovery. Anal Chem. 2009; 81(1):56–66. Epub 2008/12/04. https://doi.org/10.1021/ac8011544 PMID: 19049366.

41. Guo W, Jiang C, Yang L, Li T, Liu X, Jin M, et al. Quantitative Metabolomic Profiling of Plasma, Urine, and Liver Extracts by (1)H NMR Spectroscopy Characterizes Different Stages of Atherosclerosis in Hamsters. J Proteome Res. 2016; 15(10):3500–10. Epub 2016/08/30. https://doi.org/10.1021/acs.jproteome.6b00179 PMID: 27570155.

42. Jiang CY, Yang KM, Yang L, Miao ZX, Wang YH, Zhu HB. A (1)H NMR-Based Metabonomic Investigation of Time-Related Metabolic Trajectories of the Plasma, Urine and Liver Extracts of Hyperlipidemic Hamsters. PLoS One. 2013; 8(6):e66786. Epub 2013/07/11. https://doi.org/10.1371/journal.pone.0066786 PMID: 23840531

43. Rangan GK, Tesch GH. Quantification of renal pathology by image analysis. Nephrology (Carlton). 2007; 12(6):553–8. Epub 2007/11/13. https://doi.org/10.1111/j.1440-1797.2007.00855.x PMID: 17995580.

44. Murphy JC, Fox JG, Niemi SM. Nephrotic syndrome associated with renal amyloidosis in a colony of Syrian hamsters. J Am Vet Med Assoc. 1984; 185(11):1359–62. Epub 1984/12/01. PMID: 6511583.

45. Ramezani A, Raj DS. The gut microbiome, kidney disease, and targeted interventions. J Am Soc Nephrol. 2014; 25(4):657–70. Epub 2013/11/16. https://doi.org/10.1681/ASN.2013080905 PMID: 24231662

46. Tang WH, Wang Z, Kennedy DJ, Wu Y, Buffa JA, Agatisa-Boyle B, et al. Gut microbiota-dependent trimethylamine N-oxide (TMAO) pathway contributes to both development of renal insufficiency and mortality risk in chronic kidney disease. Circ Res. 2015; 116(3):448–55. Epub 2015/01/20. https://doi.org/10.1161/CIRCRESAHA.116.305360 PMID: 25599331

47. Ortiz GG, Bitzer-Quintero OK, Zárate CB, Rodríguez-Reynoso S, Larios-Arceo F, Velázquez-Brizuela IE, et al. Monosodium glutamate-induced damage in liver and kidney: a morphological and biochemical approach. Biomedicine & Pharmacotherapy. 2006; 60(2):86–91. https://doi.org/10.1016/j.biopha.2005.07.012.

48. Chowdhury SS, Lecomte V, Erlich JH, Maloney CA, Morris MJ. Paternal High Fat Diet in Rats Leads to Renal Accumulation of Lipid and Tubular Changes in Adult Offspring. Nutrients. 2016; 8(9). Epub 2016/08/27. https://doi.org/10.3390/nu8090521 PMID: 27563922

49. Bratoeva K, Stoyanov GS, Merdzhanova A, Radanova M. Manifestations of Renal Impairment in Fructose-induced Metabolic Syndrome. Cureus. 2017; 9(11):e1826. Epub 2018/01/13. https://doi.org/10.7759/cureus.1826 PMID: 29321950

50. van Timmeren MM, van den Heuvel MC, Bailly V, Bakker SJ, van Goor H, Stegeman CA. Tubular kidney injury molecule-1 (KIM-1) in human renal disease. J Pathol. 2007; 212(2):209–17. Epub 2007/05/02. https://doi.org/10.1002/path.2175 PMID: 17471468.

51. Chen Q, Guan X, Zuo X, Wang J, Yin W. The role of high mobility group box 1 (HMGB1) in the pathogenesis of kidney diseases. Acta Pharm Sin B. 2016; 6(3):183–8. Epub 2016/05/14. https://doi.org/10.1016/j.apsb.2016.02.004 PMID: 27175328

52. Barrios C, Beaumont M, Pallister T, Villar J, Goodrich JK, Clark A, et al. Gut- Microbiota-Metabolite Axis in Early Renal Function Decline. PLoS One. 2015; 10(8):e0134311. Epub 2015/08/05. https://doi.org/10.1371/journal.pone.0134311 PMID: 26241311

53. Feng ZM, Li TJ, Wu L, Xiao DF, Blachier F, Yin YL. Monosodium L-Glutamate and Dietary Fat Differently Modify the Composition of the Intestinal Microbiota in Growing Pigs. Obes Facts. 2015; 8(2):87–100. Epub 2015/03/21. https://doi.org/10.1159/000380889 PMID: 25791341

54. Jiang S, Xie S, Lv D, Wang P, He H, Zhang T, et al. Alteration of the gut microbiota in Chinese population with chronic kidney disease. Sci Rep. 2017; 7(1):2870. Epub 2017/06/08. https://doi.org/10.1038/s41598-017-02989-2 PMID: 28588309

55. Buckel W, Barker HA. Two pathways of glutamate fermentation by anaerobic bacteria. J Bacteriol. 1974; 117(3):1248–60. Epub 1974/03/01. PMID: 4813895

56. Gryp T, Vanholder R, Vaneechoutte M, Glorieux G. p-Cresyl Sulfate. Toxins (Basel). 2017; 9(2). Epub 2017/02/02. https://doi.org/10.3390/toxins9020052 PMID: 28146081

57. Kikuchi K, Saigusa D, Kanemitsu Y, Matsumoto Y, Thanai P, Suzuki N, et al. Gut microbiome-derived phenyl sulfate contributes to albuminuria in diabetic kidney disease. Nat Commun. 2019; 10(1):1835. Epub 2019/04/25. https://doi.org/10.1038/s41467-019-09735-4 PMID: 31015435

58. Khan TJ, Ahmed YM, Zamzami MA, Mohamed SA, Khan I, Baothman OAS, et al. Effect of atorvastatin on the gut microbiota of high fat diet-induced hypercholesterolemic rats. Sci Rep. 2018; 8(1):662. Epub 2018/01/14. https://doi.org/10.1038/s41598-017-19013-2 PMID: 29330433

59. Luo Q, Cheng D, Huang C, Li Y, Lao C, Xia Y, et al. Improvement of Colonic Immune Function with Soy Isoflavones in High-Fat Diet-Induced Obese Rats. Molecules. 2019; 24(6). Epub 2019/03/27. https://doi.org/10.3390/molecules24061139 PMID: 30909396

60. Zachariah S, Kumar K, Lee SWH, Choon WY, Naeem S, Leong C. Chapter 7—Interpretation of Laboratory Data and General Physical Examination by Pharmacists. In: Thomas D, editor. Clinical Pharmacy Education, Practice and Research: Elsevier; 2019. p. 91–108.

61. Turner PV. The role of the gut microbiota on animal model reproducibility. Animal Model Exp Med. 2018; 1(2):109–15. Epub 2019/03/21. https://doi.org/10.1002/ame2.12022 PMID: 30891555

62. Franklin CL, Ericsson AC. Microbiota and reproducibility of rodent models. Lab Anim (NY). 2017; 46 (4):114–22. Epub 2017/03/23. https://doi.org/10.1038/laban.1222 PMID: 28328896

63. Mbakwa CA, Penders J, Savelkoul PH, Thijs C, Dagnelie PC, Mommers M, et al. Gut colonization with *Methanobrevibacter smithii* is associated with childhood weight development. Obesity (Silver Spring). 2015; 23(12):2508–16. Epub 2015/11/03. https://doi.org/10.1002/oby.21266 PMID: 26524691

64. Kovesdy CP, Furth SL, Zoccali C, World Kidney Day Steering C. Obesity and Kidney Disease: Hidden Consequences of the Epidemic. Can J Kidney Health Dis. 2017; 4:2054358117698669. Epub 2017/05/26.

65. Mathur R, Kim G, Morales W, Sung J, Rooks E, Pokkunuri V, et al. Intestinal *Methanobrevibacter smithii* but Not Total Bacteria Is Related to Diet-Induced Weight Gain in Rats. Obesity. 2012; 21(4):748–54.

66. Jakobsson HE, Rodriguez-Pineiro AM, Schutte A, Ermund A, Boysen P, Bemark M, et al. The composition of the gut microbiota shapes the colon mucus barrier. EMBO Rep. 2015; 16(2):164–77. Epub 2014/12/20. https://doi.org/10.15252/embr.201439263 PMID: 25525071

67. Patra A, Mandal S, Samanta A, Chandra Mondal K, Nandi DK. Therapeutic potential of probiotic *Lactobacillus plantarum* AD3 on acetaminophen induced uremia in experimental rats. Clinical Nutrition Experimental. 2018; 19:12–22. https://doi.org/10.1016/j.yclnex.2018.02.002.

68. Eidi F, Poor -reza Gholi F, Ostadrahimi A, Dalili N, Samadian F, Barzegari A. Effect of *Lactobacillus rhamnosus* on serum uremic toxins (phenol and P-Cresol) in hemodialysis patients: A double blind randomized clinical trial. Clinical Nutrition ESPEN. 2018; 28:158–64. https://doi.org/10.1016/j.clnesp.2018.08.010. PMID: 30390875

69. Sun J, Qiao Y, Qi C, Jiang W, Xiao H, Shi Y, et al. High-fat-diet-induced obesity is associated with decreased antiinflammatory *Lactobacillus reuteri* sensitive to oxidative stress in mouse Peyer's patches. Nutrition. 2016; 32(2):265–72. Epub 2015/12/02. https://doi.org/10.1016/j.nut.2015.08.020 PMID: 26620713.

70. Kong C, Gao R, Yan X, Huang L, Qin H. Probiotics improve gut microbiota dysbiosis in obese mice fed a high-fat or high-sucrose diet. Nutrition. 2019; 60:175–84. Epub 2019/01/06. https://doi.org/10.1016/j.nut.2018.10.002 PMID: 30611080.

71. Hsu CN, Lu PC, Lo MH, Lin IC, Chang-Chien GP, Lin S, et al. Gut Microbiota- Dependent Trimethylamine N-Oxide Pathway Associated with Cardiovascular Risk in Children with Early-Stage Chronic Kidney Disease. Int J Mol Sci. 2018; 19(12). Epub 2018/11/25. https://doi.org/10.3390/ijms19123699 PMID: 30469463

72. Li D, Kirsop J, Tang WH. Listening to Our Gut: Contribution of Gut Microbiota and Cardiovascular Risk in Diabetes Pathogenesis. Curr Diab Rep. 2015; 15(9):63. Epub 2015/07/26. https://doi.org/10.1007/s11892-015-0634-1 PMID: 26208694

73. Sun G, Yin Z, Liu N, Bian X, Yu R, Su X, et al. Gut microbial metabolite TMAO contributes to renal dysfunction in a mouse model of diet-induced obesity. Biochem Biophys Res Commun. 2017; 493(2):964–70. Epub 2017/09/25. https://doi.org/10.1016/j.bbrc.2017.09.108 PMID: 28942145.

74. Watanabe H, Miyamoto Y, Honda D, Tanaka H, Wu Q, Endo M, et al. p-Cresyl sulfate causes renal tubular cell damage by inducing oxidative stress by activation of NADPH oxidase. Kidney Int. 2013; 83 (4):582–92. Epub 2013/01/18. https://doi.org/10.1038/ki.2012.448 PMID: 23325087.

75. Visconti A, Le Roy CI, Rosa F, Rossi N, Martin TC, Mohney RP, et al. Interplay between the human gut microbiome and host metabolism. bioRxiv. 2019:561787. https://doi.org/10.1101/561787

76. Ramezani A, Nolin TD, Barrows IR, Serrano MG, Buck GA, Regunathan-Shenk R, et al. Gut Colonization with Methanogenic Archaea Lowers Plasma Trimethylamine N-oxide Concentrations in Apolipoprotein e-/- Mice. Sci Rep. 2018; 8(1):14752. Epub 2018/10/05. https://doi.org/10.1038/s41598-018-33018-5 PMID: 30283097